CME LIVE OPEN ACCESS

Chemistry Research and Practice

Research Article ISSN: 3065-906X

Dialkyl Substituent Effects on the Interaction of Imidazolium Ionic Liquids with POPC Membranes by Molecular Dynamics

Leandro Segat [1*], Luís Alberto Loureiro dos Santos[1] and Hubert Stassen[2]

[1]*Federal University of Rio Grande do Sul, School of Engineering, Department of Materials, Biomaterials Laboratory, Porto Alegre, Brazil.*

[2]*Federal University of Rio Grande do Sul, Institute of Chemistry, Department of Physical Chemistry, Theoretical Chemistry Group, Porto Alegre, Brazil*

Corresponding Author: Leandro Segat, Federal University of Rio Grande do Sul, School of Engineering, Department of Materials, Biomaterials Laboratory, Porto Alegre, Brazil.

Received: 2025 Dec 08 **Accepted:** 2025 Dec 27 **Published:** 2026 Jan 06

Abstract

We employed molecular dynamics computer simulations to examine the effect of a second alkyl group on the cations of imidazolium-based ionic liquids on the properties of a fully hydrated POPC membrane. While maintaining a fixed hexadecyl group on the cations, a second methyl, butyl, and octyl group were considered. In any case, the cations rapidly inserted into the bilayer, maintaining membrane integrity without structural disruption. Radial distribution functions and density profiles indicate that an increase in the second alkyl chain on the cation favors a configuration with deeper insertion. The presence of the cations promotes structural perturbations in the lipid area and bilayer thickness, particularly the cation with the butyl substituent, while preserving the hydration of the polar region of the bilayer without promoting water penetration into the lipophilic region.

Keywords: Ionic Liquids, Phospholipid Bilayer, Bilayer Structure, Molecular Dynamics Simulation, Imidazolium-Based Ionic Liquids and Dialkyl Imidazolium

1. Introduction

Ionic liquids (ILs) are widely recognized as ionic compounds that remain liquid at relatively low temperatures below 100°C [1-4]. In addition to their characteristic thermal stability and low volatility, these compounds permit to tune their physicochemical properties by structural modifications in both, cations and anions, as well as by combining diverse cations and anions [5-21]. This structural adaptability has facilitated the development of ILs for more sophisticated applications [22]. ILs can be applied in a variety of fields, including agriculture and cosmetics, where their surfactant properties can be exploited to alter interfacial tension, wettability, and emulsion stability. Another potential application lies in medicine, pharmacology, and biochemistry, where their amphiphilic properties, affinity for lipid membranes, and micellization can be exploited to develop new drugs, treatments, and drug delivery models [22-28]. Thefore, it becomes necessary to address significant challenges related with their potentially toxic interactions with living organisms [29,30]. The growing interest in biological applications of ILs has emerged in part as a response to environmental concerns associated with the ecotoxicity of certain IL classes [29,30]. Particular attention has been given to the cytotoxicity of imidazolium-based ILs, which stems from their strong interactions with phospholipid membranes in cellular structures [31-33].

The cytotoxic effects of imidazolium ILs appear directly correlated with their membrane-disrupting capabilities. Experimental studies have demonstrated that these cations intercalate into lipid bilayers, inducing perturbations that range from moderate fluidity alterations to complete membrane disintegration, depending on their specific molecular architecture [31-35]. A comprehensive understanding of these interaction mechanisms is essential for developing safe pharmaceutical and medical applications of ILs [31,34]. Cytotoxicity assessments across various biological systems, including antifungal and bactericidal tests as well as mammalian cell exposure studies, have revealed that both, cation-anion combinations and alkyl chain lengths, play crucial roles in determining toxicity profiles [1,36,37]. These observed structure-activity relationships highlight the need for more detailed mechanistic studies on IL-membrane interactions.

Recent advances in computational chemistry have provided valuable theoretical insights into the interactions between imidazolium ILs and phospholipid bilayers [38-40]. Current

computational models primarily focus on two aspects: the structural modifications induced in the bilayer and the molecular mechanisms governing cation insertion and stabilization within membranes. The stabilization of incorporated cations appears to involve both electrostatic interactions with phosphate groups and hydrophobic effects mediated by alkyl side chains [38-40]. However, these studies describe in general dialkylated cations with a fixed methyl group[41]. Dialkyl-substituted variants remain relatively unexplored. The presence of two longer alkyl chains may significantly alter both, the insertion dynamics and the membrane perturbation patterns, due to additional steric constraints in the polar headgroup region.

This work uses atomistic molecular dynamics simulations to investigate the role of side chain (n) length changes in 1-hexadecyl-3-n-alkylimidazolium cations. Our goal is to analyze how the length of the second alkyl chain influences the way the cation inserts and organizes itself in the 1-palmitoyl-2-oleoyl-sn-glycero-3-phosphocholine (POPC) bilayer and, consequently, affects the membrane's structural properties. The simulations provide atomic-level insights into the interaction mechanisms, contributing to a fundamental understanding of the cytotoxicity of these ionic liquids and aiding in the rational design of compounds with controlled toxicity profiles for biological applications.

2. Materials and Methods

We performed molecular dynamics simulations on systems containing a hydrated POPC phospholipid bilayer composed of 128 lipids (64 per leaflet) incorporating 1-hexadecyl-3-nalkyl-imidazolium cations using the GROMACS 2024.5 software package [42]. Each simulated system contained the solvated bilayer along with one ion pair, with the cationic component consisting of [C_{16}MIM] (1-hexadecyl-3-methylimidazolium), [C_{16}BIM] (1-hexadecyl-3-butylimidazolium), or [C_{16}OIM] (1-hexadecyl-3-octylimidazolium), and the chloride (Cl^-) anion. The molecular structures of the utilized cations are presented in figure1. The equilibrated POPC bilayer system has been obtained from the Slipids database, with the ionic liquid structures and force fields generated following the AMBER protocol methodology [43-45]. This approach ensured proper system preparation while maintaining consistency with established computational chemistry standards for membrane simulations.

The simulation box model, with dimensions of 6 x 6 x 7 nm, containing the solvated POPC bilayer is a system provided already balanced and duly verified by the developers of the Slipids website for use by the scientific community. The assembly of the system with the presence of ILs was performed by the gmx insert-molecules module of the GROMACS software, where the insertion of cations and anions was performed randomly in the aqueous medium of the system with the removal of water molecules from the system for the entry of the structure of the components of each IL, thus preventing the insertion of cations into the system from occurring with overlapping of the ILs on the lipids of the bilayer, promoting an erroneous representation of the initial packing of the membrane.

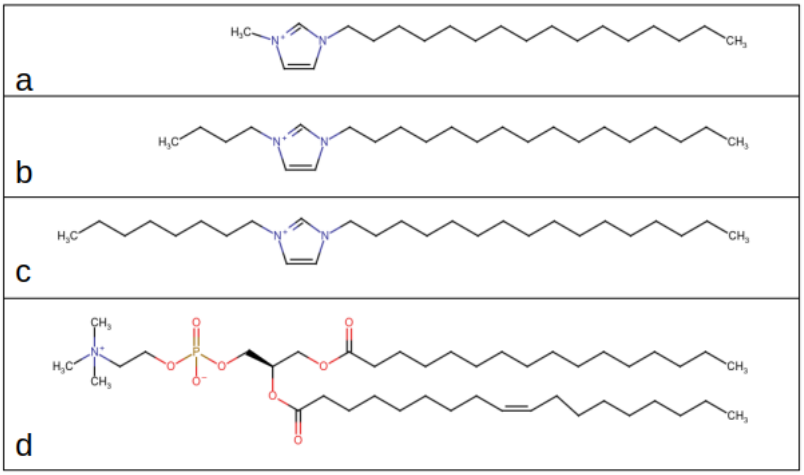

Figure 1: Structural Representations of: (a) C16MIM Cation, (b) C16BIM Cation, (c) C16OIM Cation and (d) POPC

The simulations were conducted in the isothermal-isobaric (NPT) ensemble with integration step of 0.002 fs. Temperature was maintained at 303 K using the velocity-rescaling algorithm [46]. The pressure was regulated at 1 bar by the Parrinello-Rahman barostat operating in semi-isotropic mode [47]. Three-dimensional periodic boundary conditions were implemented with a 1.4 nm cutoff radius for intermolecular interactions. Long-range electrostatic interactions were calculated using the Particle Mesh Ewald (PME) method with an identical 1.4 nm cutoff distance [48]. The LINCS algorithm [49] was employed to maintain all chemical bond constraints throughout the simulations.

The AMBER force field was selected for molecular representations in the simulations with water molecules modeled described by the TIP3P potential [50]. Ionic pairs were randomly inserted into the hydrated bilayer simulation boxes. Prior to production runs, all systems underwent potential energy minimization using the steepest descent algorithm, followed by two stages of temperature equilibration in NVT and pressure in NPT.. Subsequently, simulations were carried out for 100 ns of production

time with one cation inserted into the bilayer systems [51]. A reference system consisting solely of a hydrated phospholipid bilayer without ionic liquids was subjected to identical simulation protocols and analysis procedures for comparative purposes.All results presented in this work were obtained in triplicate.

3. Results and Discussions

Along the simulations of the bilayer systems containing Ils, we observed in any case the insertion of the cations from the water phase into the phospholipid bilayer, while the chloride anion remains solvated in the aqueous medium without interacting with the other components. Afterwards, we extended the simulations up to 100 ns monitoring the convergence of the area per phospholipid (APL) and interactions energies between cations and bilayer molecules. The final 10 ns of each trajectory have been utilized to compute the results presented in the following. A snapshot of the final configuration for each system is presented in figure 2.

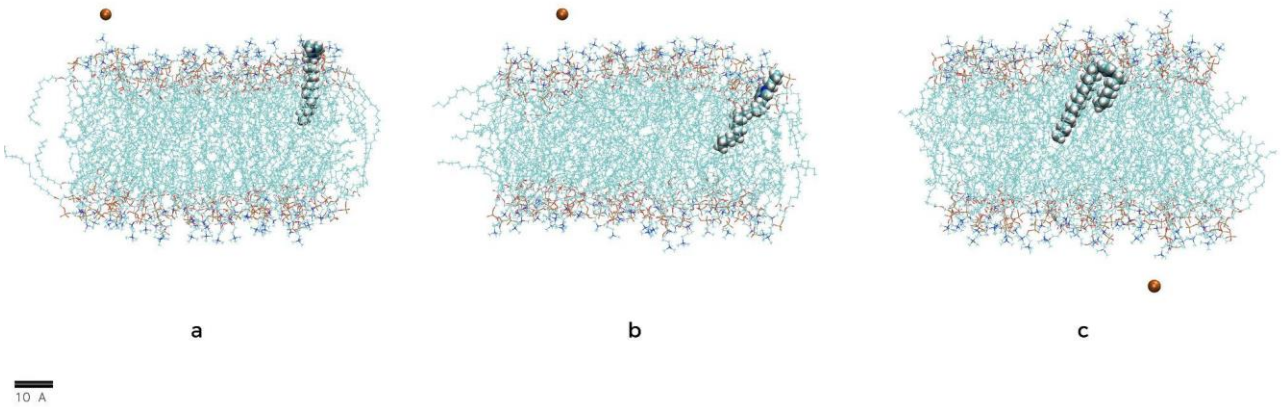

Figure 2: Cations Inserted into the Bilayer at the end of the Simulation. A) c16mim, b) c16bim and c) c16oim .Chloride Anion in Orange, Water was Removed from the Representation for Better Visualization of the System of Interest

At a glance, we observe the configurations of cations inserted into the bilayer. The [C_{16}OIM] cation inserts both alkyl chains into the hydrophobic environment of the bilayer. The [C_{16}BIM] cation, containing the shorter butyl chain (4 carbons), can not fully insert the second substituent into the hydrophobic domain, leaving it closer to the polar headgroups at the membrane surface. As expected , [C_{16}MIM] directs only the long alkyl chain towards the membrane's center [52].

Radial pair distribution functions (RDFs) for distances between the center of the imidazolium ring and three distinct atoms of POPC's polar head group have been computed. We have chosen the nitrogen atom of the choline group (N), the phosphorous (P), and the innermost oxygen (O) of the glycerol backbone to monitor changes in the coordination of the imidazolium ring within the membrane's polar region. The RDFs are illustrated in figure 3.

The C16MIM cation exhibits greater interaction with the P atom present in lipids, presenting the most predicted interaction peak and greater interaction stability. The C16BIM cation exhibits the same interaction profile as that presented for C16MIM, but with lower intensity, which can be attributed to lower insertion stability with less defined interactions. Finally, the C16OIM cation exhibits a different RDF profile, showing greater interaction with oxygen 32, which is located in the deepest region of the membrane's polar surface. This result demonstrates that the presence of the secondary octyl substituent promotes deeper insertion of the ring and, consequently, of the cation as a whole into the bilayer. These results are presented as density profiles in Figure 4, showing the greater insertion depth obtained by another analysis.

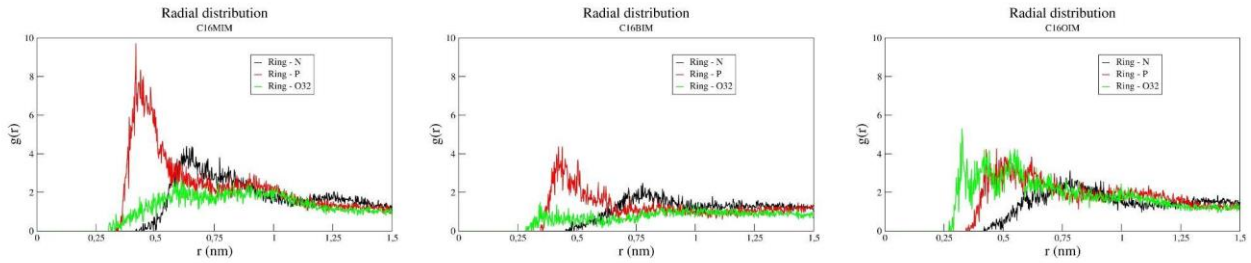

Figure 3: RDFs Between Cation Rings of all Cations and Atoms of the Head Group of POPC's Phospholipids. a) C16MIM Cation, b) C16BIM Cation and c) C16OIM Cation

Figure 4 shows the density profiles obtained for the center of mass of the ring and the last carbon of hexadecyl chain relative to the center of the membrane along the z axis. This data corroborates what was observed in Figure 3, where the increase in the lateral secondary chain promotes a deeper insertion of the ring between the head groups of the membrane and consequently a greater depth of penetration of the main side chain.

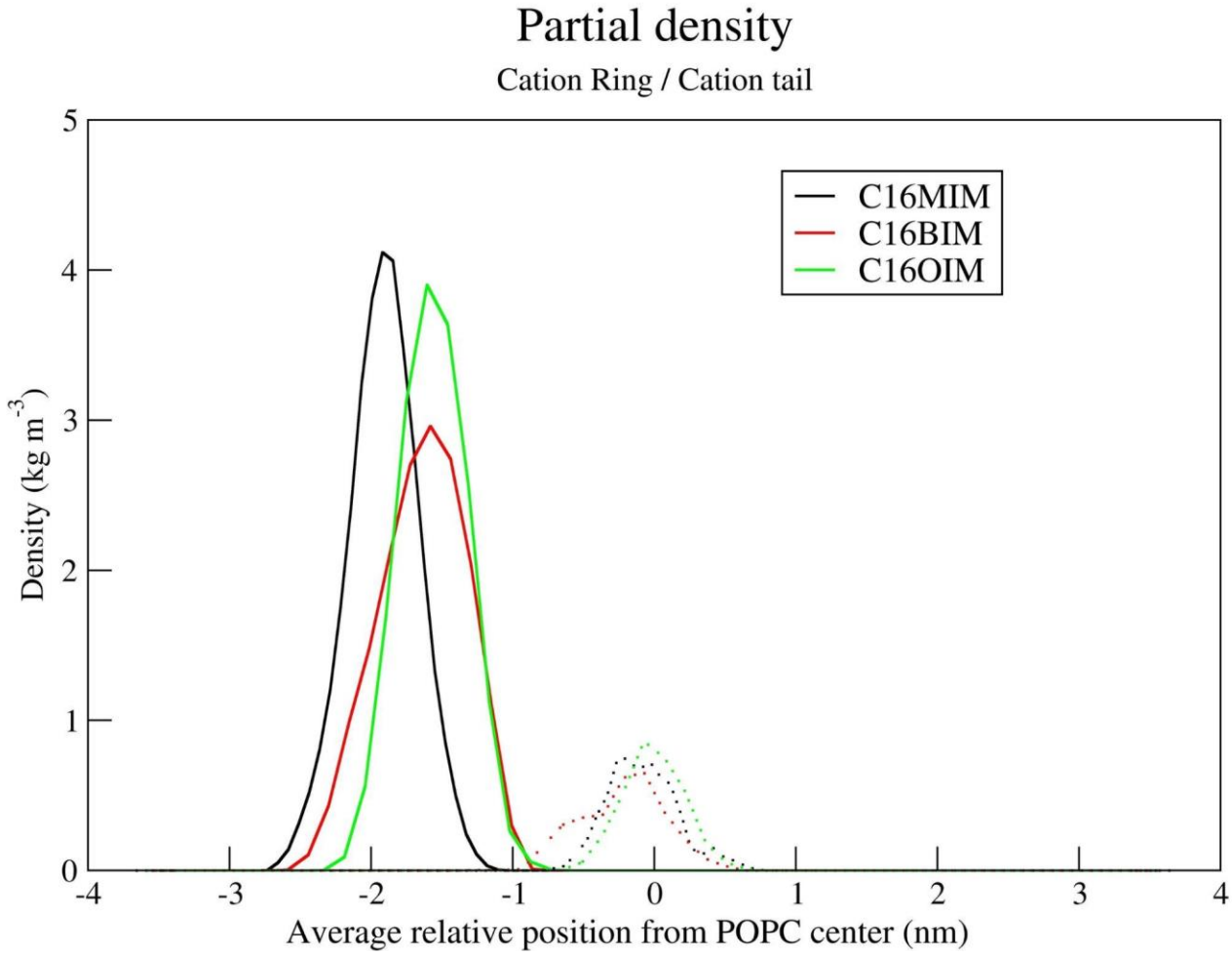

Figure 4: Density Profile for the Center of Mass of the Ring Present in the Cations and Terminal Carbon of 16 Carbon Chain Along the z Axis with the System Centered on the Membrane. Solid line for Rings and Dotted lines for Terminal Carbons

An analysis of the positioning of the secondary methyl, butyl, and octyl groups relative to membrane insertion is shown in Figure 5, where we can observe the insertion of the octyl group of the C16OIM cation by the presence of a stable density peak near the center of the membrane. When observing the methyl and butyl groups of the C16MIM and C16BIM cations, we can note a well-defined peak for the methyl group, while the butyl group presents a broader and less defined profile, indicating instability in its positioning on the membrane surface.

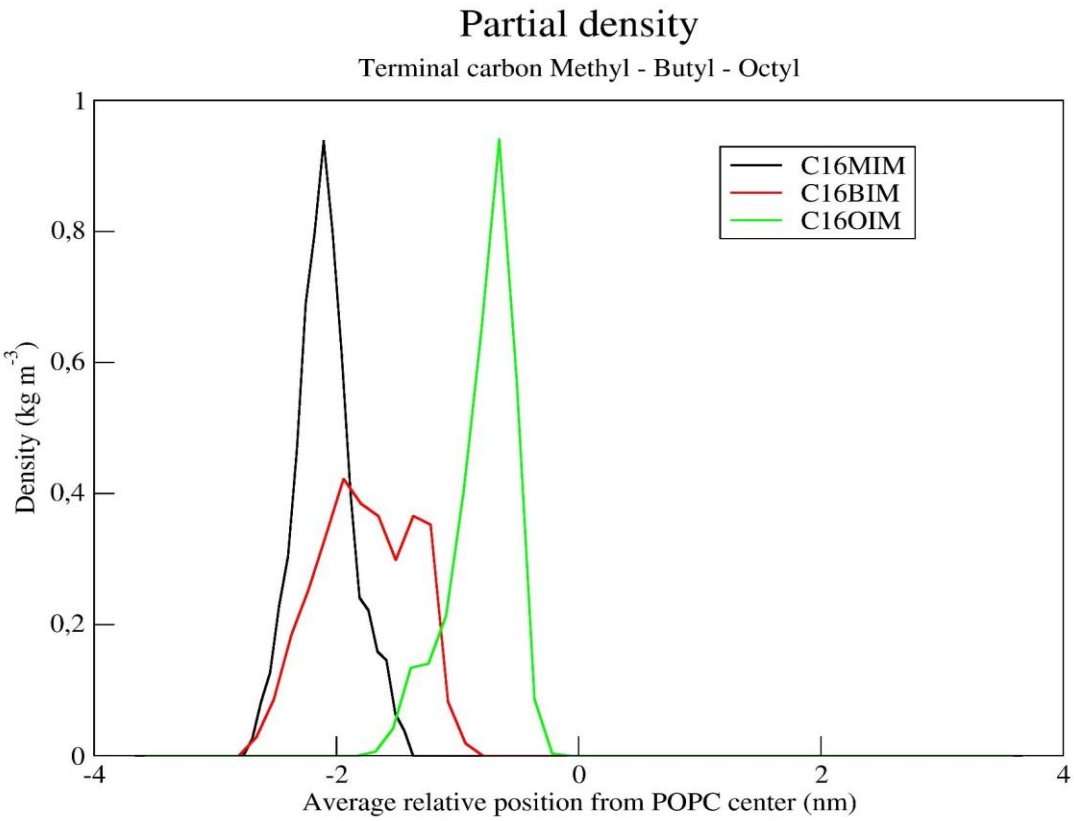

Figure 5: Density Profile for the Terminal Carbon Present in the Methyl, Butyl and Octyl Substituents Present in the Cations Along the z Axis with the System Centered in the Membrane

Figure 6 shows a comparison of the cations inserted into the membrane through MSD measurements produced by the gmx MSD module and a subgraph, derived from the MSD plot, showing the lateral diffusion coefficients of each molecule. It is possible to observe greater mobility for the C16BIM cation, followed by C16MIM and C16OIM. This greater mobility of the C16BIM cation can be translated as lower stability upon insertion, which may be related to the destabilization that occurs in the interaction between the secondary side chain (butyl) and the polar groups on the membrane surface.

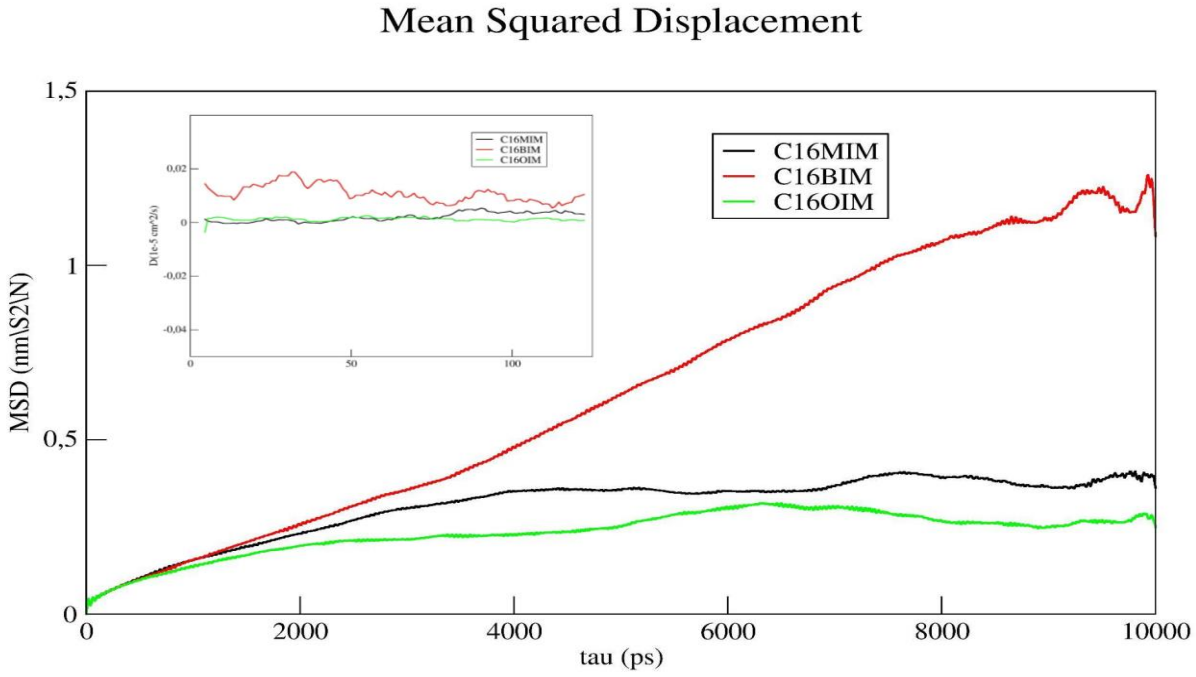

Figure 6: Mean Square Displacement and Lateral Diffusion Coefficient for Cations Inserted and Stabilized in the Membrane

Citation: Segat, L., Santos, L. A. L. S., Stassen, H. (2026). Dialkyl Substituent Effects on the Interaction of Imidazolium Ionic Liquids with POPC Membranes by Molecular Dynamics. *Chem Rec Pract, 3*(1), 01-11.

Figure 7 and 8 presents RDFs between water molecules and the aforementioned headgroup atoms of the bilayer and water densities along the z-axis with the system centered on the membrane obtained by the gmx density module. Comparing these functions and density profiles demonstrates no significant changes in the hydration patterns of the membrane surface. These results indicate that the cation insertion does not promote water intrusion into the bilayer's hydrophobic domain, preserving the membrane's fundamental barrier properties despite the structural perturbations caused by the ionic liquids. It is worth noting that for the C16BIM cation there is a situ increase in the presence of water towards the center of the membrane, but without access to the hydrophobic core of the structure. This effect may result in the non-insertion of the second side chain and its conformational instability in the presence of polar groups at the water-membrane interface, promoting destabilization of the interface and allowing a greater presence of water between the membrane head groups.

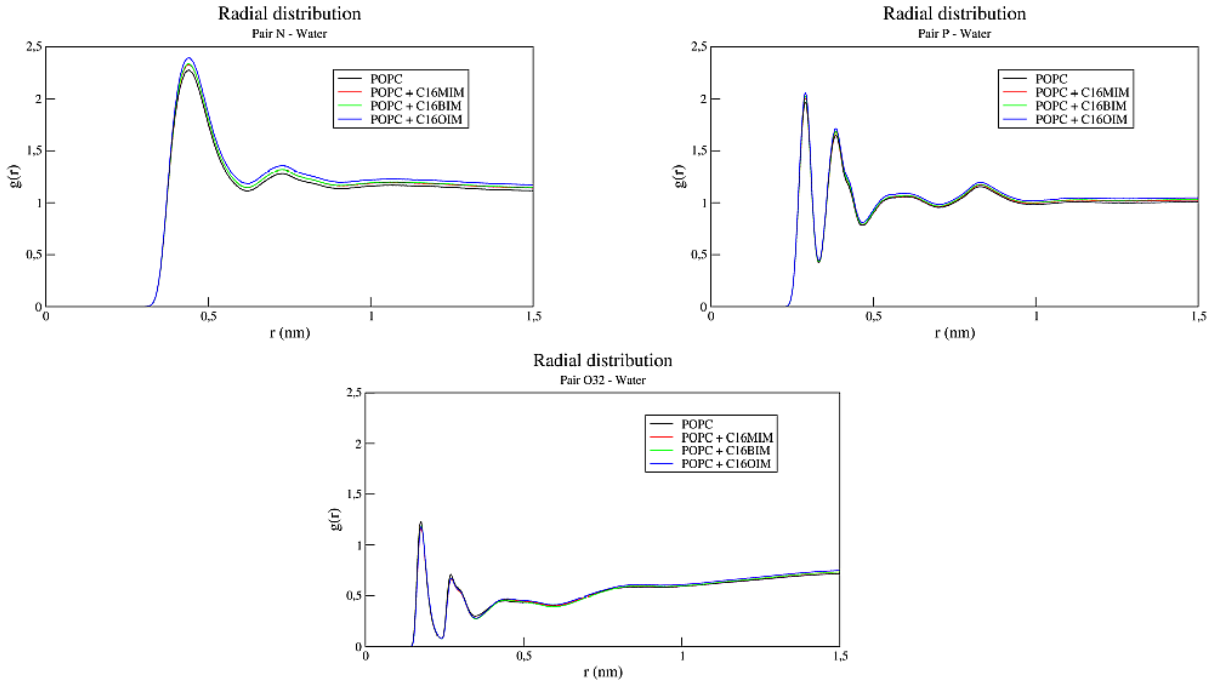

Figure 7: RDFs Between Atoms of the Polar Surface of the Bilayer and Water Molecules

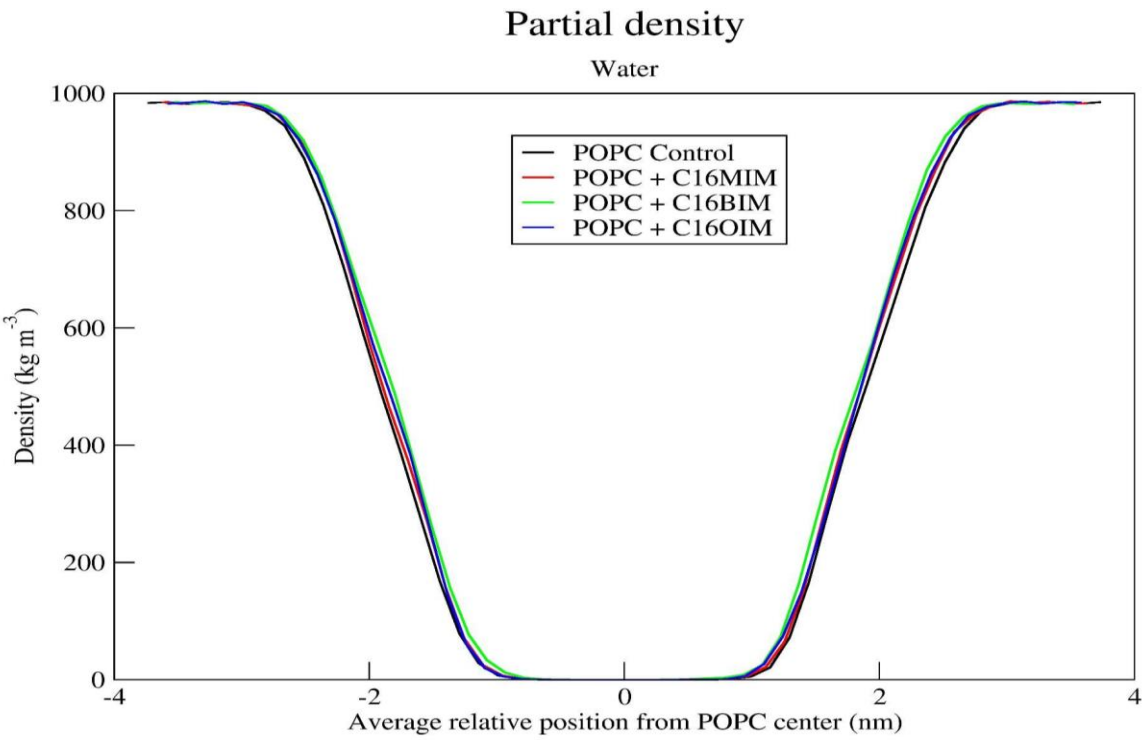

Figure 8: Water Density Profiles Along the Z-Axis Keeping the System Centered on the Membrane

The interaction energy between the cations and the phospholipid molecules has been separated into contributions stemming from Lennard-Jones and Coulomb interactions as depicted in Figure 9. More negative values in this analysis indicate stronger contributions to the overall interaction energy within the system. The total interaction energy is increased by adding more atoms to the cations as one might expect. The electrostatic contributions are mostly due to interactions of the cation's ring and the head group atoms of the membrane and are almost the same for the three cations.

On the other side, increasing the second alkyl chain in the cations comes along with enhanced Lennard-Jones interactions. A large fraction of these van der Waals type interactions reflects the hydrophobic interactions between the alkyl chains of the cations and the lipid tails and, therefore, grows strongly with larger alkyl groups in the cations. For the C16BIM cation, it is possible to observe a slight reduction in the Coulomb interaction and a slight increase in the Lennard-Jones interaction, where the increase in the L-J interaction is expected due to the increase in the non-polar presence in the cation, while the decrease in the Coulomb interaction results from the destabilization of the polar interactions between the cation ring and the lipid head groups, destabilization resulting from the non-insertion of the butyl substituent in the membrane and the persistence of a non-polar structure in a predominantly polar region where the interactions between the ring and head groups are located.

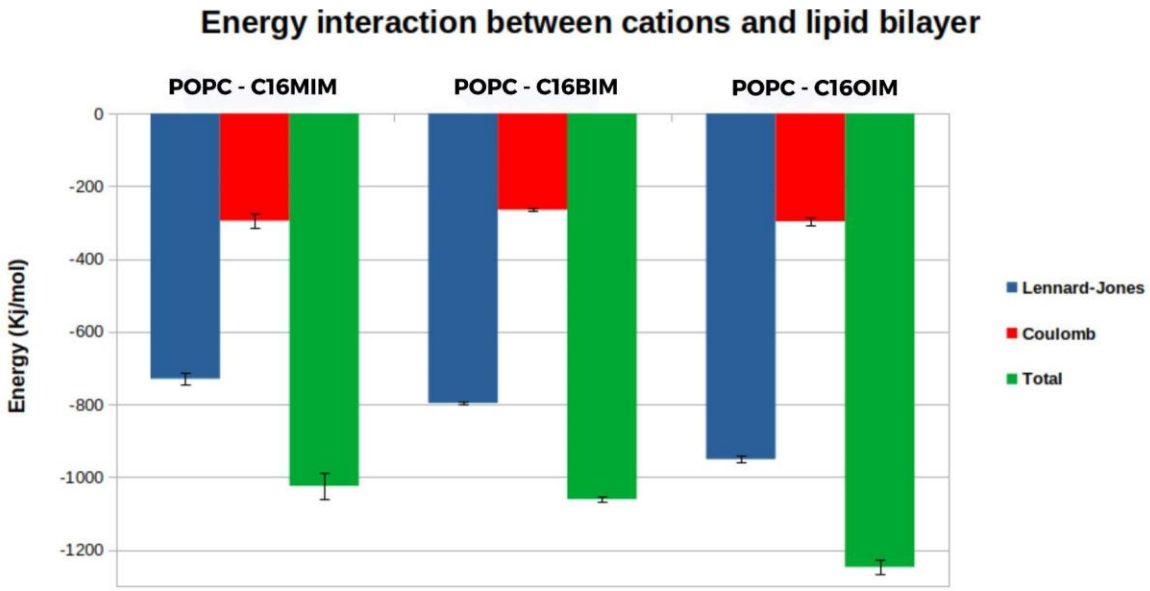

Figure 9: Average Energy Contributions of Lennard-Jones and Coulomb Interactions to the Potential Energy of the System over the 100 ns of Simulation and their Sum with Error Bars

In table 1, we have summarized several structural data for the bilayer in comparison with the unperturbed POPC bilayer. We focused on the area per phospholipid (APL) and the membrane's thickness computed with the APL@Voro post-processing software [53].

	APL (nm^2)	Thickness (nm)
POPC	0.6617 ± 0.0024	3.7218 ± 0.0026
POPC + C16MIM	0.6488 ± 0.0035	3.7660 ± 0.0004
POPC + C16BIM	0.6718 ± 0.0046	3.1439 ± 0.0132
POPC +C16OIM	0.6521 ± 0.0021	3.7319 ± 0.0044
POPC + C16OIM (4 cations)	0.6908 ± 0.0032	3.6556 ± 0.0094

Table 1: Structural Modifications in the Bilayer Promoted by the Insertion of Cations

The APL and thickness of the unperturbed bilayer are in agreement with literature data [54]. All results were obtained with a 95% confidence interval, and all variations compared to the control values were significant. The area per lipid was slightly affected by an increase of approximately 0.1 nm^2 for the C16MIM and C16OIM cations, while the C16BIM cation affected it in the same magnitude but with a decrease in APL. The most affected structural characteristic was membrane thickness, where the C16MIM and C16OIM cations promoted an increase of 0.04 and 0.01 nm, respectively, while the C16BIM cation promoted a decrease of 0.58 nm in thickness. The data do not indicate a trend of perturbation with increasing secondary side chain size, but they clearly show that the C16BIM cation, with its butyl side chain,

presented the greatest perturbation in membrane thickness. The membrane structural results obtained for the C16MIM cation are in good agreement with values reported in the literature[36] for studies involving smaller monoalkylated cations such as C12MIM, showing that the new data generated for dialkylated cations have good reliability. An additional analysis was performed by computing the structural effects of four cations inserted into the same bilayer leaflet for the C16OIM model. Increasing the concentration causes this system to follow the opposite behavior of the system with only one cation, promoting an increase in the area per lipid and a decrease in the bilayer thickness.

In Figure 10, we illustrate the deuterium order parameter for the unsaturated (left panel) and saturated (right panel) alkyl chains of the POPC molecules calculated with the gmx order module of the GROMACS software. This is a measurement of the angle of displacement perpendicular to the membrane of the carbons of the lipid tails indicating the ordering of the tails and consequently representing structural properties of the bilayer related to lipid packing. This measurement is performed by creating specific index files for one of the tails of each lipid called Sn1 and Sn2 and calculating the angles with the gmx order module present in the gromacs software. The presence of the cations quite generally reduces slightly the order parameter affecting more the carbons close to the membrane's head group than those close to the membrane's center, where Sn1 segments are slightly more affected than Sn2. We can observe that for Sn1, the insertion of the C16BIM cation promotes a more significant change in the structure in the region closest to the head groups. This effect is related to the large decrease in membrane thickness, and the fact that the greatest disturbance occurs close to the head group is related to the destabilization of the membrane surface promoted by the presence of the Butyl substitution at the interface.

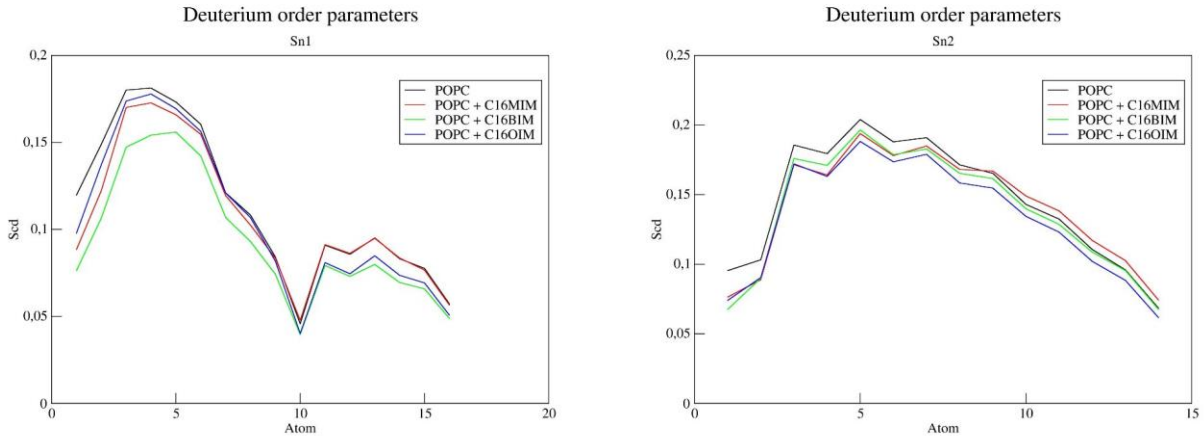

Figure 10: Deuterium Order Parameters for the Sn1 (Left Panel) and Sn2 (Right Panel) Alkyl Chains of POPC

4. Conclusions

Ionic liquids based on the imidazolium cation containing a fixed hexadecyl substituent and a substituent ranging from methyl, butyl, and octyl with chloride as the counterion were inserted into hydrated POPC phospholipid bilayers. 100-nanosecond MD simulations were performed to evaluate the cation insertion configuration and the structural effects of the insertion on the bilayer. Cation stabilization in the membrane occurs through nonpolar interactions within the bilayer between the carbon chains of the cations and lipids and through polar interactions at the membrane surface between the phospholipid head groups and the rings present on the cations. Cations with sufficiently large secondary side chains (octyl) are capable of doubly inserting into the bilayer, resulting in deeper insertion than cations with smaller side chains. On the other hand, cations with intermediate side chains (butyl) do not insert twice, and the secondary chain remains unstable between the bilayer's nonpolar head groups, destabilizing the region, resulting in the largest structural perturbations with significant compression of the bilayer thickness. Under the conditions of the study, no significant change in the membrane-water interface was observed, with no water penetration into the bilayer or membrane disruption. The result presented for the increase in the number of C16OIM cations shows a sharp change in membrane perturbation behavior, indicating that concentration effects should be explored in future studies. The work may demonstrate that the second side chain influences the depth of cation insertion and the perturbation promoted in the membrane structure, providing new perspectives for the study focus in modeling and ILs for biological fields.

Funding: This study was financed in part by the Coordenação de Aperfeiçoamento de Pessoal de Nível Superior – Brasil (CAPES) – Finance Code 001.

Ethics Statement: not applicable.

Consent to Publish Declaration: not applicable.

Consent to Participate Declaration: not applicable.

Acknowledgments: Federal University of Rio Grande do Sul, the Department of Materials (DEMAT), the Institute of Chemistry and the Group of Computational Theoretical

Chemistry for all the support provided and the infrastructure provided.

Abbreviations:

The following abbreviations are used in this manuscript:
IL's: Ionic liquids
POPC: 1-palmitoyl-2-oleoyl-sn-glycero-3-phosphocholine
C16MIM: 1-Hexadecyl-3 -Methylimidazolium
C16BIM: 1-Hexadecyl-3 -Butylimidazolium
C16OIM: 1-Hexadecyl-3-Octylimidazolium
MD: Molecular dynamics
APL: Area per lipid
RDF: Radial pair distribution functions
NPT: Isothermal-isobaric ensemble
PME: Particle Mesh Ewald

References

1. Walden, P. (1914). Molecular weights and electrical conductivity of several fused salts. *Bull. Acad. Imper. Sci. (St. Petersburg), 1800*.
2. Chum, H. L., Koch, V. R., Miller, L. L., & Osteryoung, R. A. (1975). Electrochemical scrutiny of organometallic iron complexes and hexamethylbenzene in a room temperature molten salt. *Journal of the American Chemical Society, 97*(11), 3264-3265.
3. áDe Long, H. C. (1994). Structure of 1-ethyl-3-methylimidazolium hexafluorophosphate: model for room temperature molten salts. *Journal of the Chemical Society, Chemical Communications*, (3), 299-300.
4. Wilkes, J. S., & Zaworotko, M. J. (1992). Air and water stable 1-ethyl-3-methylimidazolium based ionic liquids. *Journal of the Chemical Society, Chemical Communications,* (13), 965-967.
5. Fredlake, C. P., Crosthwaite, J. M., Hert, D. G., Aki, S. N., & Brennecke, J. F. (2004). Thermophysical properties of imidazolium-based ionic liquids. *Journal of Chemical & Engineering Data, 49*(4), 954-964.
6. Raabe, G., & Köhler, J. (2008). Thermodynamical and structural properties of imidazolium based ionic liquids from molecular simulation. *The Journal of chemical physics, 128*(15).
7. Weingärtner, H. (2008). Understanding ionic liquids at the molecular level: facts, problems, and controversies. *Angewandte Chemie International Edition, 47*(4), 654-670.
8. Zhang, S., Sun, N., He, X., Lu, X., & Zhang, X. (2006). Physical properties of ionic liquids: database and evaluation. *Journal of physical and chemical reference data, 35*(4), 1475-1517.
9. Bonhote, P., Dias, A. P., Papageorgiou, N., Kalyanasundaram, K., & Grätzel, M. (1996). Hydrophobic, highly conductive ambient-temperature molten salts. *Inorganic chemistry, 35*(5), 1168-1178.
10. Perini, L. S., Dos Santos, L. A. L., & Stassen, H. K. (2025). Dialkyl Substituent Effects on the Interaction of Imidazolium Ionic Liquids with POPC Membranes by Molecular Dynamics.
11. McEwen, A. B., Ngo, H. L., LeCompte, K., & Goldman, J. L. (1999). Electrochemical properties of imidazolium salt electrolytes for electrochemical capacitor applications. *Journal of the Electrochemical Society, 146*(5), 1687.
12. Hyun, B. R., Dzyuba, S. V., Bartsch, R. A., & Quitevis, E. L. (2002). Intermolecular dynamics of room-temperature ionic liquids: femtosecond optical Kerr effect measurements on 1-alkyl-3-methylimidazolium bis ((trifluoromethyl) sulfonyl) imides. *The Journal of Physical Chemistry A, 106*(33), 7579-7585.
13. Every, H. A., Bishop, A. G., MacFarlane, D. R., Orädd, G., & Forsyth, M. (2004). Transport properties in a family of dialkylimidazolium ionic liquids. *Physical Chemistry Chemical Physics, 6*(8), 1758-1765.
14. Huddleston, J. G., Visser, A. E., Reichert, W. M., Willauer, H. D., Broker, G. A., & Rogers, R. D. (2001). Characterization and comparison of hydrophilic and hydrophobic room temperature ionic liquids incorporating the imidazolium cation. *Green chemistry, 3*(4), 156-164.
15. Tsuzuki, S., Tokuda, H., Hayamizu, K., & Watanabe, M. (2005). Magnitude and directionality of interaction in ion pairs of ionic liquids: Relationship with ionic conductivity. *The Journal of Physical Chemistry B, 109*(34), 16474-16481.
16. Fitchett, B. D., Knepp, T. N., & Conboy, J. C. (2004). 1-Alkyl-3-methylimidazolium bis (perfluoroalkylsulfonyl) imide water-immiscible ionic liquids: the effect of water on electrochemical and physical properties. *Journal of the Electrochemical Society, 151*(7), E219.
17. McFarlane, D. R., Sun, J., Golding, J., Meakin, P., & Forsyth, M. (2000). High conductivity molten salts based on the imide ion. *Electrochimica Acta, 45*(8-9), 1271-1278.
18. Hyk, W., Caban, K., Donten, M., & Stojek, Z. (2001). Properties of microlayers of ionic liquids generated at microelectrode surface in undiluted redox liquids. *Part II. The Journal of Physical Chemistry B, 105*(29), 6943-6949.
19. Earle, M. J., Esperança, J. M., Gilea, M. A., Canongia Lopes, J. N., Rebelo, L. P., Magee, J. W., ... & Widegren, J. A. (2006). The distillation and volatility of ionic liquids. *Nature, 439*(7078), 831-834.
20. Zaitsau, D. H., Kabo, G. J., Strechan, A. A., Paulechka, Y. U., Tschersich, A., Verevkin, S. P., & Heintz, A. (2006). Experimental vapor pressures of 1-alkyl-3-methylimidazolium bis (trifluoromethylsulfonyl) imides and a correlation scheme for estimation of vaporization enthalpies of ionic liquids. *The Journal of Physical Chemistry A, 110*(22), 7303-7306.
21. Köddermann, T., Paschek, D., & Ludwig, R. (2008). Ionic liquids: Dissecting the enthalpies of vaporization. *ChemPhysChem, 9*(4), 549-555.
22. Egorova, K. S., Gordeev, E. G., & Ananikov, V. P. (2017). Biological activity of ionic liquids and their application in pharmaceutics and medicine. *Chemical reviews, 117*(10), 7132-7189.
23. Kapitanov, I. V., Jordan, A., Karpichev, Y., Spulak, M., Perez, L., Kellett, A., ... & Gathergood, N. (2019). Synthesis, self-assembly, bacterial and fungal toxicity, and preliminary biodegradation studies of a series of L-phenylalanine-derived surface-active ionic liquids. *Green Chemistry, 21*(7), 1777-1794.

24. Wojcieszak, M., Syguda, A., Lewandowska, A., Marcinkowska, A., Siwinska-Ciesielczyk, K., Wilkowska, M., ... & Materna, K. (2023). Synthesis and surface properties of piperidinium-based herbicidal ionic liquids as a potential tool for weed control. *Journal of Agricultural and Food Chemistry, 71*(11), 4550-4560.
25. Šarac, B., Medoš, Ž., Cognigni, A., Bica, K., Chen, L. J., & Bešter-Rogač, M. (2017). Thermodynamic study for micellization of imidazolium based surface active ionic liquids in water: effect of alkyl chain length and anions. *Colloids and Surfaces A: Physicochemical and Engineering Aspects, 532,* 609-617.
26. Szaniawska, M., Szymczyk, K., Zdziennicka, A., & Jańczuk, B. (2023). Thermodynamic parameters of berberine with Kolliphor mixtures adsorption and micellization. *Molecules, 28*(7), 3115.
27. Ray, G. B., Chakraborty, I., Ghosh, S., Moulik, S. P., & Palepu, R. (2005). Self-aggregation of alkyltrimethylammonium bromides (C10-, C12-, C14-, and C16TAB) and their binary mixtures in aqueous medium: a critical and comprehensive assessment of interfacial behavior and bulk properties with reference to two types of micelle formation. *Langmuir, 21*(24), 10958-10967.
28. Yuli, I., Tzafrir, I., & Salama, P. (2023). Compatibility investigation of cationic surfactants with anionic species. *Cosmetics, 10*(2), 45.
29. Wei, P., Pan, X., Chen, C. Y., Li, H. Y., Yan, X., Li, C., ... & Yan, B. (2021). Emerging impacts of ionic liquids on eco-environmental safety and human health. *Chemical Society Reviews, 50*(24), 13609-13627.
30. Liu, R., Shi, Y., Zhang, R., & Dai, F. (2019). Progress in environmental behaviors and safety of ionic liquids. *Chinese Sci. Bull, 64*, 3158-3164.
31. Galluzzi, M., Marfori, L., Asperti, S., De Vita, A., Giannangeli, M., Caselli, A., ... & Podestà, A. (2022). Interaction of imidazolium-based ionic liquids with supported phospholipid bilayers as model biomembranes. *Physical Chemistry Chemical Physics, 24*(44), 27328-27342.
32. Fernandes, M. M., Carvalho, E. O., Correia, D. M., Esperança, J. M., Padrão, J., Ivanova, K., ... & Lanceros-Mendez, S. (2022). Ionic liquids as biocompatible antibacterial agents: a case study on structure-related bioactivity on Escherichia coli. *ACS applied bio materials, 5*(11), 5181-5189.
33. Flieger, J., & Flieger, M. (2020). Ionic liquids toxicity—benefits and threats. *International Journal of Molecular Sciences, 21*(17), 6267.
34. Gupta, R., Sharma, V. K., Gupta, J., & Ghosh, S. K. (2022). 1, 3 Dialkylated Imidazolium Ionic Liquid Causes Interdigitated Domains in a Phospholipid Membrane. *Langmuir, 38*(11), 3412-3421.
35. Hitaishi, P., Raval, M., Seth, A., Kumar, S., Mithu, V. S., Sharma, V. K., & Ghosh, S. K. (2023). Cholesterol-controlled interaction of ionic liquids with model cellular membranes. *Langmuir, 39*(27), 9396-9405.
36. Sharma, V. K., Ghosh, S. K., García Sakai, V., & Mukhopadhyay, R. (2020). Enhanced microscopic dynamics of a liver lipid membrane in the presence of an ionic liquid. *Frontiers in chemistry, 8*, 577508.
37. Klähn, M., & Zacharias, M. (2013). Transformations in plasma membranes of cancerous cells and resulting consequences for cation insertion studied with molecular dynamics. *Physical Chemistry Chemical Physics, 15*(34), 14427-14441.
38. Bingham, R. J., & Ballone, P. (2012). Computational study of room-temperature ionic liquids interacting with a POPC phospholipid bilayer. *The Journal of Physical Chemistry B, 116*(36), 11205-11216.
39. Lee, H. (2015). Effects of imidazolium-based ionic surfactants on the size and dynamics of phosphatidylcholine bilayers with saturated and unsaturated chains. *Journal of Molecular Graphics and Modelling, 60,* 162-168.
40. Lim, G. S., Jaenicke, S., & Klähn, M. (2015). How the spontaneous insertion of amphiphilic imidazolium-based cations changes biological membranes: a molecular simulation study. *Physical Chemistry Chemical Physics, 17*(43), 29171-29183.
41. Kumar, S., Scheidt, H. A., Kaur, N., Kang, T. S., Gahlay, G. K., Huster, D., & Mithu, V. S. (2019). Effect of the alkyl chain length of amphiphilic ionic liquids on the structure and dynamics of model lipid membranes. *Langmuir, 35*(37), 12215-12223.
42. Berendsen, H. J., van der Spoel, D., & van Drunen, R. (1995). GROMACS: A message-passing parallel molecular dynamics implementation. *Computer physics communications, 91*(1-3), 43-56.
43. Jambeck, J. P., & Lyubartsev, A. P. (2012). An extension and further validation of an all-atomistic force field for biological membranes. *Journal of chemical theory and computation, 8*(8), 2938-2948.
44. De Andrade, J., Böes, E. S., & Stassen, H. (2002). Computational study of room temperature molten salts composed by 1-alkyl-3-methylimidazolium cations force-field proposal and validation. *The journal of physical chemistry B, 106*(51), 13344-13351.
45. de Andrade, J., Böes, E. S., & Stassen, H. (2002). A force field for liquid state simulations on room temperature molten salts: 1-ethyl-3-methylimidazolium tetrachloroaluminate. *The Journal of Physical Chemistry B, 106*(14), 3546-3548.
46. Bussi, Giovanni, Davide Donadio, and Michele Parrinello. "Canonical sampling through velocity rescaling." The Journal of chemical physics 126.1 (2007).
47. Parrinello, M., & Rahman, A. (1981). Polymorphic transitions in single crystals: A new molecular dynamics method. *Journal of Applied physics, 52*(12), 7182-7190.
48. Essmann, U., Perera, L., Berkowitz, M. L., Darden, T., Lee, H., & Pedersen, L. G. (1995). A smooth particle mesh Ewald method. *The Journal of chemical physics, 103*(19), 8577-8593.
49. Hess, B., Bekker, H., Berendsen, H. J., & Fraaije, J. G. (1997). LINCS: A linear constraint solver for molecular simulations. *Journal of computational chemistry, 18*(12), 1463-1472.
50. Jorgensen, W. L., Chandrasekhar, J., Madura, J. D., Impey, R. W., & Klein, M. L. (1983). Comparison of simple potential functions for simulating liquid water. *The*

Journal of chemical physics, 79(2), 926-935.

51. Perini, L. S., Dos Santos, L. A. L., & Stassen, H. K. (2025). Dialkyl Substituent Effects on the Interaction of Imidazolium Ionic Liquids with POPC Membranes by Molecular Dynamics.
52. Lee, H., & Jeon, T. J. (2015). The binding and insertion of imidazolium-based ionic surfactants into lipid bilayers: The effects of the surfactant size and salt concentration. *Physical Chemistry Chemical Physics, 17*(8), 5725-5733.
53. Lukat, G., Krüger, J., & Sommer, B. (2013). APL@ Voro: a Voronoi-based membrane analysis tool for GROMACS trajectories. *Journal of chemical information and modeling, 53*(11), 2908-2925.
54. Grote, F., & Lyubartsev, A. P. (2020). Optimization of slipids force field parameters describing headgroups of phospholipids. *The Journal of Physical Chemistry B, 124*(40), 8784-8793.